Reaction Chemistry & Engineering

PAPER

View Article Online
View Journal | View Issue

Cite this: *React. Chem. Eng.*, 2019, 4, 2156

Synthesis of menthol from citronellal over supported Ru- and Pt-catalysts in continuous flow†

Muhammad Azkaar,[a] Päivi Mäki-Arvela,[a] Zuzana Vajglová,[a] Vyacheslav Fedorov,[ab] Narendra Kumar,[a] Leena Hupa,[a] Jarl Hemming,[a] Markus Peurla,[a] Atte Aho[a] and Dmitry Yu Murzin *[a]

One-pot menthol synthesis from citronellal in a trickle bed reactor was investigated using Ru/H-beta-300 zeolite extrudates without any binder and Pt- and Ru-extrudates containing 70 wt% H-beta-25 zeolites and 30 wt% bentonite binder using different methods of metal loading on the extrudates. The catalytic results were correlated with the physico-chemical properties of bifunctional zeolite-based extrudates. The conversion of citronellal to menthol was nearly the same for Pt extrudates being independent of catalyst acidity or the metal particle size. Ru extrudates also exhibited similar conversion levels as a function of time-on-stream, except for very mildly acidic Ru/beta-300 extrudates, which gave much lower conversion. Pt extrudates showed better stability with time on stream in comparison with Ru extrudates. The best catalyst giving the highest menthol yield and a low amount of acyclic hydrogenation products was Ru-beta-bentonite extrudates where Ru was located randomly in the mixture of 70% H-beta-25 and 30% bentonite binder. Hydrogenation was more prominent for Pt than for Ru catalysts, most probably due to their higher hydrogenation ability. Stereoselectivity to menthol varied in the trickle bed reactor in the range of 67 to 73%. In a batch reactor for Ru- and Pt-catalysts independent of support acidity, it was in the range of 70–71%. The reuse of Ru/H-beta-300 extrudates was successfully demonstrated.

Received 22nd August 2019,
Accepted 24th October 2019

DOI: 10.1039/c9re00346k

rsc.li/reaction-engineering

1 Introduction

Menthol, a monoterpene alcohol, is an essential compound for the pharmaceutical and flavouring industries because of its cooling effects and minty fragrance. It has been extracted in the form of essential oil for medicinal purposes in China for centuries.[1] Menthol is widely used as an important flavouring agent in many daily life products such as toothpaste, soaps, shampoos, chewing gum, and cosmetics.[1]

Menthol is produced globally from both natural and synthetic routes. As the world demand for menthol increases, the same holds for its production which leads to anticipation of a shortage of natural resources. The very first industrial process for the chemical synthesis of menthol in 1970 (ref. 2) was based on catalytic hydrogenation of thymol using Ru/Al_2O_3 as a catalyst followed by subsequent fractional distillation to separate (+,−)-menthols from other isomers. The overall yield of this process exceeds 90% after many recycling steps. Another method to produce menthol is *via* the transformation of myrcene into diethylgeranylamine (DGA) by adding diethylamine in the presence of a lithium catalyst. Thereafter, DGA is isomerized to chiral citronellal, which in turn is cyclized to isopulegol in the presence of zinc bromide. Isopulegol is further hydrogenated in the presence of a nickel catalyst to menthol.[2]

Currently, several research groups globally are active in one-pot synthesis of menthol from citronellal by using heterogeneous catalysts.[3–17] Two reaction steps are involved in this process: cyclization of citronellal to isopulegol and hydrogenation of the latter to menthol.[3] Bifunctional catalysts, having an acidic support for cyclization and the metal function for hydrogenation, are used to catalyse these reactions. Suitable catalysts are active and selective towards menthol formation, avoiding at the same time side reactions such as citronellal hydrogenation, dimerization, and defunctionalization.[4]

One-pot synthesis of menthol from citronellal was investigated in detail by Plösser *et al.*,[4] Cortes *et al.*[3] and Mertens *et al.*[5] On the other hand, Mäki-Arvela *et al.*[6] studied menthol synthesis over heterogeneous catalysts using citral as a starting material. The selectivity towards menthols over 2.0 wt% Pt on beta zeolites was more than 95% as reported by

[a] *Johan Gadolin Process Chemistry Centre, Åbo Akademi University, Turku/Åbo, Finland. E-mail: dmurzin@abo.fi*
[b] *Saint-Petersburg State Institute of Technology (Technical University), St. Petersburg, Russia*

† Electronic supplementary information (ESI) available. See DOI: 10.1039/c9re00346k

Mertens *et al.*[5] According to their research, Pt is more chemoselective towards the desired hydrogenation as compared to Pd and other metals. Plösser *et al.*[4] reported 1.0 wt% Ru on beta zeolites as the best catalyst for the transformation of citronellal to menthol resulting in a menthol selectivity of more than 93%. The catalyst was highly diastereoselective towards racemic menthol as compared to other catalysts having Pt or Pd as the metal. In the kinetic study of the one-pot transformation of citronellal to menthols over 1% Ru/H-BEA-25, it was shown that at lower temperatures the consecutive hydrogenation of citronellal prevails, whereas at high temperatures defunctionalization of menthols is favored leading to a maximum menthol yield at 100 °C.[7] Overall, the authors reported both Ru and Pt as suitable metals for one-pot synthesis of menthol from citronellal.

In this work one-pot menthol synthesis from citronellal is demonstrated for the first time in a continuous trickle bed reactor over Pt and Ru extrudates containing beta-zeolites, which were synthesized using bentonite, an aluminium phyllosilicate natural clay as a binder. The main aim of this work was to systematically study the effect of the extrudate preparation method with controlled deposition of metal on its properties. A similar study was already conducted for *n*-hexane hydroisomerization over a Pt-catalyst.[18] In other publications of the authors, citronellal cyclization was carried out in a continuous mode over extrudates based on proton forms of beta and Y zeolites with different types of binders.[19,20] In this work, the previous studies were extended to also include hydrogenation of isopulegol. For this purpose, three different methods were used for the preparation of Pt and Ru extrudates, namely an *in situ* method, in which the metal precursor was loaded *via* the evaporation–impregnation method on a composite of beta zeolite and binder, while in the two other methods the metal precursor was introduced either on beta zeolite or on bentonite, and thereafter mixed with bentonite or beta zeolite, respectively. Extrusion and calcination were the subsequent steps in the catalyst preparation. In addition, for Pt extrudates an egg-shell type catalyst was also prepared *via* the post synthesis method, where the metal was introduced onto the shaped bodies. The catalysts were characterized by various physico-chemical methods and used in one-pot synthesis of menthol in a trickle bed reactor apparently under the influence of mass transfer limitations. As a comparison, kinetic experiments with supported Pt- and Ru-catalysts were also performed in a batch reactor under mass transfer free conditions. This work can be considered as a step towards industrial production of fine chemicals in a continuous mode using extrudates as catalysts.

2 Experimental

2.1 Chemicals

The following chemicals were used as received: cyclohexane (Alfa Aesar, ≥99.9 wt%), racemic (±)-citronellal (Sigma-Aldrich, ≥95.0 wt%), menthol (Aldrich, ≥99.0 wt%), geraniol (Lancaster, tech. quality), nerol (Sigma-Aldrich, ≥97.0 wt%), iso-menthol (Molekula), neomenthol (Fluka, ≥97.0 wt%), citronellol (Fluka, ≥99.0 wt%), isopulegol (Fluka, ≥99.0 wt%), tetrahydrofuran (Sigma-Aldrich, ≥99.9 wt%) and heptane (Sigma-Aldrich, ≥99.9 wt%).

2.2 Catalyst preparation

The two types of zeolites, NH_4-beta-25 (CP814E) and H-beta-300 (CP811C), used in this study were acquired from Zeolites International. The number at the end of each zeolite represents the SiO_2/Al_2O_3 molar ratio reflecting acidity. More specifically, a higher ratio corresponds to lower acidity. NH_4-Beta-25, supplied in an ammonium form, was transformed into the proton from *i.e.* H-beta-25 in a muffle oven using the step calcination procedure shown in Table S1.†

The synthesis of shaped Pt- and Ru-extrudates containing 30 wt% aluminosilicate clay bentonite from VWR International as a binder was the same as the previously published procedure.[18] Based on the previous studies,[18–20] the zeolite/binder weight ratio of 70/30 has been found suitable for easy shaping of the catalyst by extrusion to achieve strong and stable extrudates. All materials were crushed and sieved into a fraction <63 μm in a vibratory micro mill (Fritsch). Pt- and Ru-modified catalysts were prepared by a conventional evaporation–impregnation method. Tetraammoniumplatinum(II) nitrate ($Pt(NH_3)_4(NO_3)_2$, ≥50.0% Pt basis, Sigma-Aldrich) and ruthenium(III) chloride trihydrate ($RuCl_3 \cdot 3H_2O$, technical, Sigma-Aldrich) were used as the platinum and ruthenium precursors, respectively.

The procedure of shaped catalyst preparation included three steps, namely catalyst synthesis, impregnation of the metal and catalyst shaping (Fig. 1). All the catalysts containing the binder were prepared with a 70 : 30 ratio of H-beta-25 : bentonite and with a nominal metal loading of 2 wt% in the final extrudates. Different variations of the synthesis steps were used to prepare four different types of Pt-extrudates denoted as 2 wt% [Pt/(H-beta-25 + bentonite) post-synthesis], 2 wt% [Pt/(H-beta-25 + bentonite) *in situ*], 2 wt% [Pt/(bentonite) + H-beta-25] and 2 wt% [Pt/(H-beta-25) + bentonite], and three types of Ru-extrudates denoted as 2 wt% [Ru/(H-beta-25 + bentonite) *in situ*], 2 wt% [Ru/(bentonite) + H-beta-25] and 2 wt% [Ru/(H-beta-25) + bentonite].

2 wt% Ru/H-beta-300 extrudates were prepared without a binder from the slurry containing a different weight ratio (54.9/44.1/1.0) for the catalyst powder/distilled water/methylcellulose compared to H-beta-25 extrudates (44.5/54.5/1.0). The size of all the shaped catalysts was 1.4 mm × *ca.* 10 mm.

2.3 Catalytic experiments

One-pot menthol synthesis (Fig. 2) in a trickle bed reactor was performed with two sets of Pt and Ru shaped catalysts. For each reaction, the catalyst in the extruded form was dried in the oven at 70 °C overnight. Thereafter, 1 g of catalyst (10 × 1.4 mm) was mixed with 15 g of glass beads (0.2–0.8 mm) and loaded inside the jacketed tubular reactor (ID 12.5 mm). A catalyst amount of 1 g was chosen to achieve a citronellal

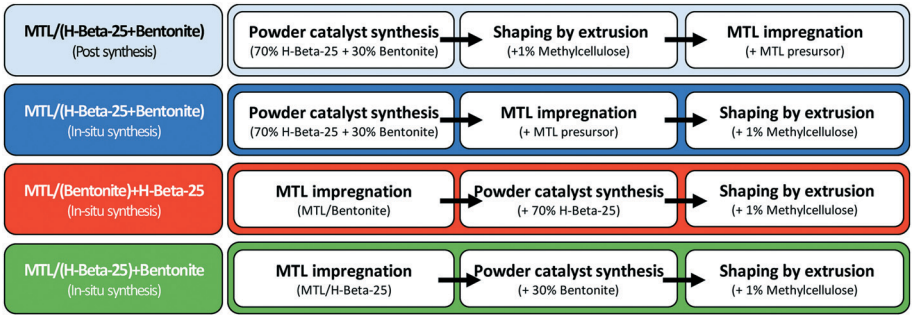

Fig. 1 Procedures for synthesis of different extrudates. *MTL – metal: Pt or Ru.

conversion of less than 100% and 15 g of glass beads was chosen to fill the whole reactor volume for better raw material distribution throughout the reactor. Ru- and Pt-catalysts were reduced *in situ* under a hydrogen flow of 50 ml min^{-1} using the temperature ramp of 10 °C min^{-1} to 350 °C for 2 h. Thereafter, the reactor was cooled down to the reaction temperature of 35 °C. After reaching the reaction temperature, the reactor and the connecting lines were flushed with deoxygenated cyclohexane for about 20 minutes with a flow rate of 0.5 ml per minute prior to the experiment. The reaction was started after pressurizing the reactor with hydrogen to 10 bar, and changing the cyclohexane flow to a mixture of 0.086 mol l^{-1} racemic (±)-citronellal in cyclohexane with a flow rate of 0.4 ml min^{-1}. The reaction was carried out for 150 minutes with sampling after every 30 minutes. *Ca.* 0.5 mL of the sample was taken at the outlet of the reactor *via* a three-way valve. During sampling, the pressure drop in the reactor was negligible. After sampling, the pressure was equalized within 1 min. After 150 minutes, the reactant flow through the reactor was stopped and switched to the solvent for flushing. The reactor was slowly depressurized to ambient pressure, heating was also stopped, and the reactor was purged with an inert gas to remove hydrogen. After disassembling the reactor system, the catalyst was dried and separated from glass beads using tweezers, and stored for characterization. During the reaction, no catalyst displacement was observed.

The catalyst reuse was investigated in the following way: the catalyst was flushed in the reactor under a flow of cyclohexane and left under 1.5 bar hydrogen pressure overnight. In the following day, the second experiment was performed with the same catalyst *via* flushing the catalyst prior to the reaction with deoxygenated cyclohexane for 20 min.

The experimental part for the batch reactor experiments is provided in the ESI.†

2.4 Analysis of liquid phase products

The liquid products were diluted with cyclohexane and analysed using an Agilent GC 6890N equipped with an FID and DB-1 column (length 30 m, internal diameter 250 μm

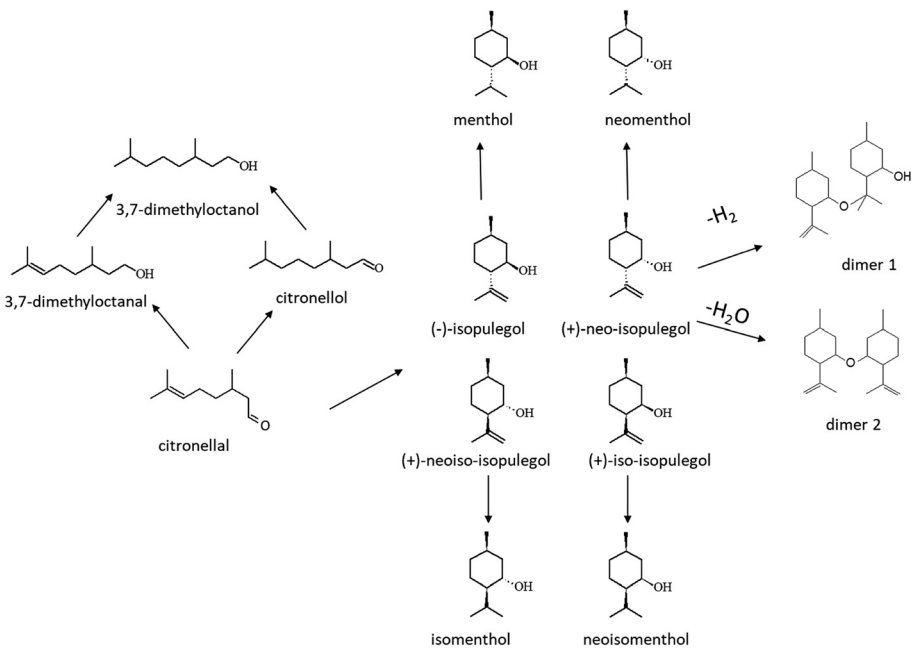

Fig. 2 Reaction scheme for one-pot synthesis of menthol from citronellal.

and film thickness 0.5 μm). The temperature program started at 110 °C followed by a temperature gradient to 130 °C at a ramp of 0.4 °C min^{-1} and then an increase to 200 °C at a ramp of 13 °C min^{-1}. The mobile phase was helium. The temperature of the FID was 340 °C. The products were confirmed with an Agilent GC/MS 6890N/5973N using a DB-1 column (length 30 m, internal diameter 250 μm and film thickness 0.5 μm).

2.5 Definitions

The conversion of the reactant was calculated by using the following equation:

$$X(\%) = \frac{C_0 - C_i}{C_0} \times 100 \quad (1)$$

where X is the conversion of the reactant at time t, %, C_0 denotes the initial molar concentration of the reactant, mol l^{-1}, and C_i is the molar concentration of the reactant at time t, mol l^{-1}.

Selectivity was calculated according to

$$S_p(\%) = \frac{C_p}{\sum (C_a + C_b + C_c + \cdots + C_z)} \times 100 \quad (2)$$

where S_p is the selectivity to product p at a certain conversion (%), and C_p is the molar concentration of product p at a particular conversion (mol l^{-1}). $C_a + C_b + C_c + \cdots + C_z$ denotes the sum of the molar concentrations of all the products at the same conversion (mol l^{-1}).

The liquid phase mass balance, *i.e.* the sum of the masses of the reactant and products visible in GC analysis was calculated using the following equation:

$$\mathrm{GCLPA}(\%) = \frac{\sum m_i}{\sum m_0} \times 100 \quad (3)$$

$\sum m_i$ = sum of mass concentrations of all components at different sampling times.

$\sum m_0$ = sum of mass concentrations of all components at time = 0.

No internal standards were used. The liquid mass balance was calculated with respect to the actual initial reactant concentration at time 0 for each experiment.

The reaction rates (r) and turnover frequency (TOF) were calculated as follows:[21]

$$r_{TB} = \frac{\Delta \dot{n}}{m_{cat}} \mathrm{mol\,s^{-1}\,g^{-1}} \quad (4)$$

$$r_B = \frac{\Delta n}{\Delta t \cdot m_{cat}} \mathrm{mol\,s^{-1}\,g^{-1}} \quad (5)$$

$$\mathrm{TOF_{TB}} = \frac{\dot{n} - \dot{n}_{out}}{n_{metal}} \mathrm{s^{-1}} \quad (6)$$

$$\mathrm{TOF_B} = \frac{\Delta n \cdot V_l}{\Delta t \cdot n_{metal}} \mathrm{s^{-1}} \quad (7)$$

where $\mathrm{TOF_{TB}}$ was obtained in the trickle-bed reactor and $\mathrm{TOF_B}$ is obtained over a powder catalyst in a batch reactor, $\Delta \dot{n}$ denotes the change in the molar flow rate of the feed in the inlet and outlet of the trickle bed reactor, $\Delta n/\Delta t$ indicates the number of reacted moles per time interval Δt in a batch reactor, m_{cat} is the catalyst mass, V_l is the liquid volume and n_{metal} is the amount of exposed moles of the catalytically active metal.

The effectiveness factor (η) and the percentage of catalyst utilization (PCU) were calculated as follows:[21]

$$\eta = \frac{r_{TB}}{r_B} \quad (8)$$

$$\mathrm{PCU} = \frac{\mathrm{TOF_{TB}}}{\mathrm{TOF_B}} \times 100 \quad (9)$$

The residence time in the trickle bed reactor (τ) was calculated to be 12.5 min according to the following equation:

$$\tau = \frac{V_{CB} \cdot \varepsilon_{CB}}{Q_{v(l)}} \quad (10)$$

where the volume of the catalyst bed V_{CB} is equal to 12.5 mL, ε_{CB} is the porosity of the catalyst bed (0.4) and $Q_{v(l)}$ is the feedstock flow rate (0.4 mL min^{-1} at room temperature).

The packed density (ρ_{CB}) and liquid hold-up (V_l) were calculated to be 1.3 g mL^{-1} and 5.9 mL, respectively, according to:

$$\rho_{CB} = \frac{m_{CB}}{V_{CB}} \quad (11)$$

$$V_l = V_R \cdot \varepsilon_{CB} \quad (12)$$

where the weight of the catalyst bed m_{CB} is equal to 16 g (1 g of catalyst + 15 g of glass bead) and the volume of the reactor V_R is equal to 14.7 mL.

2.6 Catalyst characterization methods

Nitrogen-physisorption using a Sorptometer 1900 (Carlo Erba Instruments) was used to determine the textural properties of the microporous materials. A sample was outgassed at 150 °C for 3 h before each measurement. The Dubinin equation and the Horvath–Kawazoe method were used for calculations of the specific surface area and pore volume, respectively. The measurement temperature was −196 °C.

Fourier transform infrared spectroscopy (FTIR) was used to determine the amount of Brønsted and Lewis acid sites on the catalyst with pyridine as a probe molecule (ATI Mattson FTIR Infinity Series). A powder catalyst sample of 10–20 mg was pressed into a pellet shape and loaded in the cell. Before pyridine adsorption, the catalyst was outgassed at 450 °C and 0.08 mbar pressure for two hours and the background spectrum was recorded at 100 °C. If the noise level was within acceptable limits, pyridine was then adsorbed at 100 °C for 20–30 min. The spectra were re-recorded at 100 °C after heating the catalyst at 250, 350 and 450 °C. Lewis acidity was quantified at 1450 cm^{-1} and Brønsted acidity at 1550 cm^{-1} from the respective bands. The acid strength was identified

from the temperature at which pyridine was desorbed. The concentration of acid sites was calculated using the extinction coefficient of Emeis.[22]

Scanning electron microscopy (Zeiss Leo Gemini 1530) was used to investigate the surface morphology, size, shape and chemical composition of fresh and spent catalysts. 10–15 mg of the catalyst was used for analysis on a thin film coated with activated carbon. SEM images were obtained by using an accelerating voltage of 2.7 kV with a working distance of 2–7 mm. Chemical analysis of the catalyst was done by energy dispersive X-ray microanalysis.

The metal particle size distribution was determined by transmission electron microscopy (TEM, Jeol JEM-14000 plus). Both pre-reduced fresh and spent catalysts were characterized using ImageJ software to calculate the average particle size and metal dispersion from TEM images.

Size exclusion chromatography (SEC) was applied to identify the presence of dimers and polymers trapped inside the pores or adsorbed on the catalyst surface. Adsorbed organic molecules were extracted under reflux from the spent catalyst (20 mg) using 20 ml heptane as a solvent.[23] The mixture was continuously mixed with a magnetic stirrer at 400 rpm for 4 h in the presence of a condenser at 0 °C. After extraction, the solvent was evaporated at 40 °C under nitrogen flow. The organic residue was then dissolved in 10 ml of tetrahydrofuran (THF), and the solution was filtered using a 0.2 mm membrane PTFE filter. The sample after filtration was transferred into a GC vial and analysed by SEC-HPLC with two columns, Jordi Gel DVB 500A (300 × 7.8 mm) and guard column (50 × 7.8 mm). Air pressure was set at 3.5 bar, and the temperature was kept at 40 °C.

The spent catalysts were characterized to determine their carbon, hydrogen, nitrogen, and sulphur contents. 2–3 mg of the spent catalyst was introduced in a tin container which was then folded and placed inside an auto-sampler of the ThermoFisher Scientific Flash 2000-Combustion CHNS/O analyser. The sample was oxidized in the presence of an excess of oxygen at 900 °C, and the resulting gaseous products were passed through a gas chromatographic system for analysis.

An L&W crush tester with two parallel plates (SE 048, Lorentzen & Wettre, Sweden) was used to detect the force needed for an extrudate to collapse. The mechanical strength of the extrudates was determined in the vertical and horizontal positions. For every sample, the average of ten crush tests in each position was calculated.

3 Results and discussion

3.1 Catalyst characterization

The specific surface areas and pore volumes of the extrudate catalysts (Table 1) show that the highest specific surface area was exhibited by 2 wt% Ru/H-beta-300 extrudates, not containing any binder. The second highest specific surface area in Ru extrudates was found in 2 wt% [Ru/H-beta-25 + bentonite], while the lowest one was exhibited by 2 wt% [(Ru/bentonite) + H-beta-25]. An analogous trend was observed for Pt extrudates indicating that when the metal precursor is loaded on a highly acidic beta zeolite, a higher specific surface area was obtained, which can be attributed to modifications of the zeolite upon exposure to the metal precursor. In addition, the parent bentonite exhibits a much lower specific surface area (186 m^2 g_{cat}^{-1}) than the parent H-beta-25 (681 m^2 g_{cat}^{-1}).[24] A slightly lower specific surface area was obtained for 2 wt% [Pt/(bentonite) + H-beta-25] extrudates than that for the corresponding powder mixture,[18] which can be explained by compaction during extrusion. The specific surface areas of the catalysts used in the batch reactor are shown in Table S3.† Due to a low metal loading, the specific surface areas of the Ru- and Pt-catalysts were the same or marginally lower than that for the parent material. The acidity of the catalysts determined by pyridine adsorption desorption (Table 2) shows that the extrudates prepared by different methods exhibited very different acidities. The highest Brønsted acidity was found in 2 wt% [Pt/(H-beta-25 + bentonite) post synthesis] when Pt was introduced on the shaped body, while the lowest was found in Pt/H-beta-25 which was extruded with bentonite (2 wt% [Pt/(H-beta-25) + bentonite]), clearly showing that the preparation method has a pronounced effect on acidity.[18] It is also interesting that the concentration of Brønsted acid sites in 2 wt% [Pt/(bentonite) + H-beta-25] and 2 wt% [Pt/(H-beta-25) +

Table 1 Specific surface area and pore volume of catalysts

Catalyst (extrudates)	Specific surface area (m^2 g_{cat}^{-1})	Micropore volume (cm^3 g_{cat}^{-1})	Meso- and macropore volume (cm^3 g_{cat}^{-1})	Ref.
2.0 wt% [Ru/(H-beta-25 + bentonite) *in situ*]	479	0.17	0.24	CW
2.0 wt% [Ru/(bentonite) + H-beta-25]	470	0.17	0.25	
2.0 wt% [Ru/(H-beta-25) + bentonite]	491 (207)	0.17 (0.07)	0.25 (0.22)	
2.0 wt% Ru/H-beta-300	628	0.22	0.06	
2.0 wt% [Pt/(H-beta-25 + bentonite) post]	452	0.16	0.19	8
2.0 wt% [Pt/(H-beta-25 + bentonite) *in situ*]	452 (133)	0.16 (0.05)	0.18 (0.17)	8 (CW)
2.0 wt% [Pt/(bentonite) + H-beta-25]	431	0.15	0.21	8
2.0 wt% [Pt/(H-beta-25) + bentonite]	473	0.17	0.22	

CW – current work, (spent catalyst).

Table 2 Brønsted and Lewis acid sites determined by FTIR spectroscopy, [a]experimentally found. 250 °C = sum of weak (w) + medium (m) + strong (s) acid sites, 350 °C = m + s, 450 °C = s

Catalyst (extrudates)	Brønsted acidity, μmol g^{-1}			Lewis acidity, μmol g^{-1}			TAS	
	Weak	Medium	Strong	Weak	Medium	Strong	μmol g^{-1}	Ref.
2 wt% [Pt/(H-beta-25 + bentonite), post synthesis]	54	0	129	0	1	24	208	8
2 wt% [Pt/(H-beta-25 + bentonite), *in situ* synthesis]	97	1	12	13	2	6	131	
2 wt% [Pt/(H-bentonite) + H-beta-25]	74	11	35	5	5	15	145 (265[a])	
2 wt% [Pt/(H-beta-25) + bentonite]	1	0	54	0	0	13	69 (79[a])	
2 wt% [Ru/(H-beta-25 + bentonite), *in situ* synthesis]	132	13	29	65	4	9	252	CW
2 wt% [Ru/(H-bentonite) + H-beta-25]	81	21	18	46	8	8	183	
2 wt% [Ru/(H-beta-25) + bentonite]	123	10	26	42	0	6	207	
2 wt% Ru/H-beta-300 extrudates	51	2	0	6	0	0	59	

[a] Theoretical value calculated from the contribution of non-agglomerated components,[8] CW – current work, TAS – total acid sites.

bentonite] composites is lower than the theoretical level calculated from non-agglomerated compounds.[18]

For Ru extrudates, the highest Brønsted acid site concentration was observed for 2 wt% [Ru/(H-beta-25 + bentonite) *in situ*] with Ru loaded prior to extrusion. For catalysts used in the batch reactor, the highest Brønsted acidity was determined for 2.5 wt% Pt/H-beta-25, as expected (Table S4†).

EDX results illustrate that the 2 wt% [Pt/(H-beta-25 + bentonite) post synthesis] composite catalyst is of an egg-shell type, containing Pt mostly on its surface (Table 3), while the other catalysts exhibited a metal loading close to the nominal loading with Pt more equally distributed across extrudates.[18] For Ru and Pt catalysts used in the batch reactor for comparison with continuous operation, the metal loadings were slightly different than the nominal loadings and the SiO_2/Al_2O_3 ratios as expected (Table S5†).

The platinum containing extrudates of beta zeolites with the binder possess the same structures as their parent materials as reported by Vajglová *et al.*[18] SEM-EDX results show the presence of various metals in the extrudates, namely iron and magnesium. These metals originate from bentonite, where they are present as oxides. Inhomogeneous mixing in the extrudates is visible in Fig. 3.

TEM images show that 2 wt% Ru/H-beta-300 exhibited slightly larger particles than the other Ru extrudates (Fig. 4, Table 4). The particle sizes of Pt were smaller than those of Ru. The smallest Pt particles were found in 2 wt% Pt/(bentonite) + H-beta-25, clearly showing that the preparation method of metal-extrudates has a major effect on the metal particle size.[18] After the reaction, the metal particle sizes of the spent catalysts were slightly smaller compared to those of the fresh ones (Tables 4 and S6†) indicating that no sintering occurred due to mild reaction conditions. The TEM results for the catalysts used in the batch reactor shown in Table S6 and Fig. S1† revealed that the highest metal dispersion was found in acidic 2.5 wt% Pt/H-beta-25.

The results from the extracted coke from the spent catalysts used in the trickle bed reactor showed that a larger amount of coke eluting at 14.96 min was extracted from the 2 wt% [Pt/(H-beta-25 + bentonite) *in situ*] catalyst in comparison to 2 wt% [Ru/(H-beta-25) + bentonite] (Table 5), which is not in line with the lower Brønsted acidity of the former (Table 2). Organic elemental analysis showed that the spent 2 wt% [Pt/(H-beta-25 + bentonite) *in situ*] catalyst contained more carbon than 2 wt% [Ru/(H-beta-25) + bentonite] (Table 6) in accordance with the lower GCLPA for the former catalyst (see below).

The mechanical strength of the extrudates was higher in a vertical position with random deposition of metal and lower when the metal was deposited exclusively on bentonite (Table 7). The lowest mechanical strength was observed for extrudates where the metal was deposited exclusively on H-beta zeolite. All Pt- and Ru-extrudates tested in this work as extrudates kept their shape and also their length after the reaction.

Table 3 Results from EDX analysis from the bifunctional extrudates as a function of weight percent (wt%)

Catalyst (extrudates)	SiO_2	Al_2O_3	Other elements	SiO_2/Al_2O_3	SiO_2/Pt, SiO_2/Ru	Ref.
2 wt% [Ru/(H-beta-25 + bentonite)]	87.8	9.0	Ru = 2.28 Fe_2O_3 = 0.45 MgO = 0.55	9.8	38.5	CW
2 wt% [Ru/(bentonite) + H-beta-25]	86.7	9.2	Ru = 2.59 Fe_2O_3 = 1.02 MgO = 0.43	9.4	33.5	
2 wt [Ru/(H-beta-25) + bentonite]	86.5	9.3	Ru = 3.19 Fe_2O_3 = 0.71 MgO = 0.32	9.3	27.1	
2 wt% [Pt/(H-beta-25 + bentonite) post synthesis]	81.7	8.4	Pt = 8.33 (1.45) Fe_2O_3 = 1.19 MgO = 0.36	9.7	9.8 (56.3)	8
2 wt% [Pt/(H-beta-25 + bentonite) *in situ*]	87.9	9.2	Pt = 2.31 MgO = 0.56	9.6	38.1	
2 wt% [Pt/(bentonite) + H-beta-25]	86.5	9.7	Pt = 2.61 Fe_2O_3 = 0.85 MgO = 0.39	8.9	33.1	
2 wt% [Pt/(H-beta-25) + bentonite]	87.1	8.4	Pt = 3.41 Fe_2O_3 = 0.75 MgO = 0.36	10.4	25.5	

CW – current work, (calculated Pt concentration in the entire extrudate body).

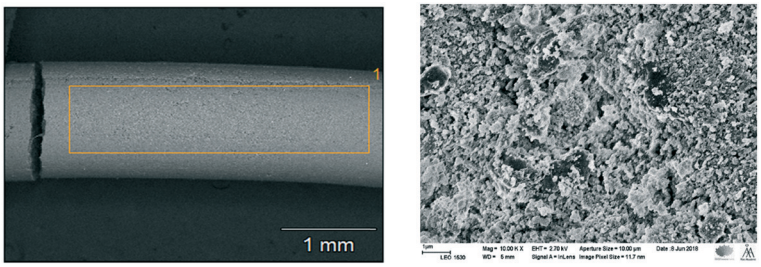

a b

Fig. 3 a) SEM micrograph of the fresh 2 wt% [Ru/(H-beta-25) + bentonite]. b) SEM micrograph of the fresh 2 wt% [Pt/(H-beta-25 + bentonite) *in situ*].

3.2 Productivity in the trickle bed reactor

In the preliminary tests, different reaction temperatures and liquid flow rates were tested in one-pot synthesis of menthol starting from citronellal. The results revealed that the suitable temperature and liquid flow rate were 35 °C and 0.4 ml min^{-1}, respectively, giving lower than 100% conversion of citronellal with 1 g of catalyst in 15 g of glass beads with a residence time of 12.5 min. Such conversion levels were specifically selected to allow comparison between catalysts and elucidation of catalyst deactivation. Evidently, at higher temperatures and longer residence time, full conversion can be easily achieved. Under the selected reaction conditions, the lowest conversion for Pt extrudates was obtained over 2 wt% [Pt/(H-beta-25 + bentonite) *in situ*] (Fig. 5a); however, the differences in citronellal conversion were quite minor when taking into account the differences in catalyst acidity (Table 2) or metal dispersion (Table 4). For Ru extrudates, the lowest conversion was obtained with mildly acidic 2 wt% Ru/H-beta-300 extrudates without a binder (Fig. 5c), while with all other catalysts the differences in conversion were minor. The conversion levels for Pt catalysts (79.6–84.5%) were, however, slightly higher than those for Ru catalysts (77.1–78.5%) (Table 8). This might be due to the fact that Pt is very active in hydrogenation already at 35 °C in comparison to Ru (see below).

Catalytic performance as a function of time-on-stream (TOS) was stable only for 2 wt% [Pt/(H-beta-25 + bentonite) *in situ*], while for the other Pt extrudates it slightly decreased with increasing TOS (Fig. 5a). Stable conversion for Ru extrudates was only observed for 2 wt% [Ru/(H-beta-25) + bentonite] (Fig. 5c). These results show that both Pt and Ru extrudates prepared by the *in situ* method from the composite comprising of H-beta-25 and bentonite exhibited the best catalyst stability. The relative error of measurements was less than ±3%.

The liquid phase mass balance closure typically increased with increasing TOS (Fig. 5b and d). Higher GCLPAs were obtained for 2 wt% Ru/H-beta-300 extrudates without a binder followed by 2 wt% [Ru/(H-beta-25 + bentonite) *in situ*] (Table 7) than those for other Ru- and Pt-catalysts containing 30 wt% bentonite binder. In addition, the lower GCLPA of 2 wt% [Pt/(H-beta-25 + bentonite) *in situ*] in comparison with the corresponding value for 2 wt% [Ru/(H-beta-25) + bentonite] is in line with organic elemental analysis and coke extraction results (Tables 5 and 6).

3.3 Comparison with batch operation

As a comparison to continuous operation, one-pot menthol synthesis was investigated in a batch reactor (Fig. S2–S5, Table S7†). The initial TOF was calculated from the moles of reacted citronellal in the first 15 min divided by the moles of exposed metal. The initial TOF of Ru/H-beta-300 was slightly lower than the corresponding value for Pt/H-beta catalysts. This result can be attributed to the lower catalytic activity of Ru at 35 °C in comparison with Pt. For Pt-catalysts, the same initial TOFs were determined despite different acidities and metal dispersions. These results are different from the literature data[4] for menthol synthesis over Ru/H-beta zeolites with different acidities and Ru-particle sizes. The authors[4] reported that the conversion of citronellal was the highest with 1.4 nm Ru particles supported on H-beta-35.

A comparison of the reaction rates for 2 wt% Ru/H-beta-300 extrudates in the trickle bed reactor and for 2.5 wt% Ru/H-beta-300 powder in the batch reactor allows elucidation of the influence of mass transfer. At 39.3% conversion in the trickle bed reactor, the rate after 90 min time on stream with 12.5 min residence time was 2.7×10^{-7} mol s^{-1} g_{cat}^{-1}, while the reaction was very rapid for the powder catalyst in the autoclave giving already 71.6% conversion and a rate of 1.88×10^{-5} mol s^{-1} g_{cat}^{-1} after 15 min. A very low catalyst effectiveness factor of 0.06 for Ru/H-beta-300 extrudates strongly suggests that in the case of continuous operation, requiring a large size of catalyst particles in the form of extrudates to avoid a high pressure drop, the catalyst productivity is much lower than that for batch operation. It should be pointed out that the effectiveness factor for 2% Ru-extrudates without a binder was somewhat approximated based on experimental results for the Ru-catalyst in the powder form with a somewhat higher metal loading of 2.5 wt% at the same conversion level of 40% with a time interval of 8.4 min (Tables 8 and S7†). The effectiveness factor of 2 wt% Pt/H-beta-25 extrudates containing the bentonite binder was calculated to be 0.13–0.14 using the results obtained over the 2.5% Pt/H-beta-25 powder catalyst without a binder at the same

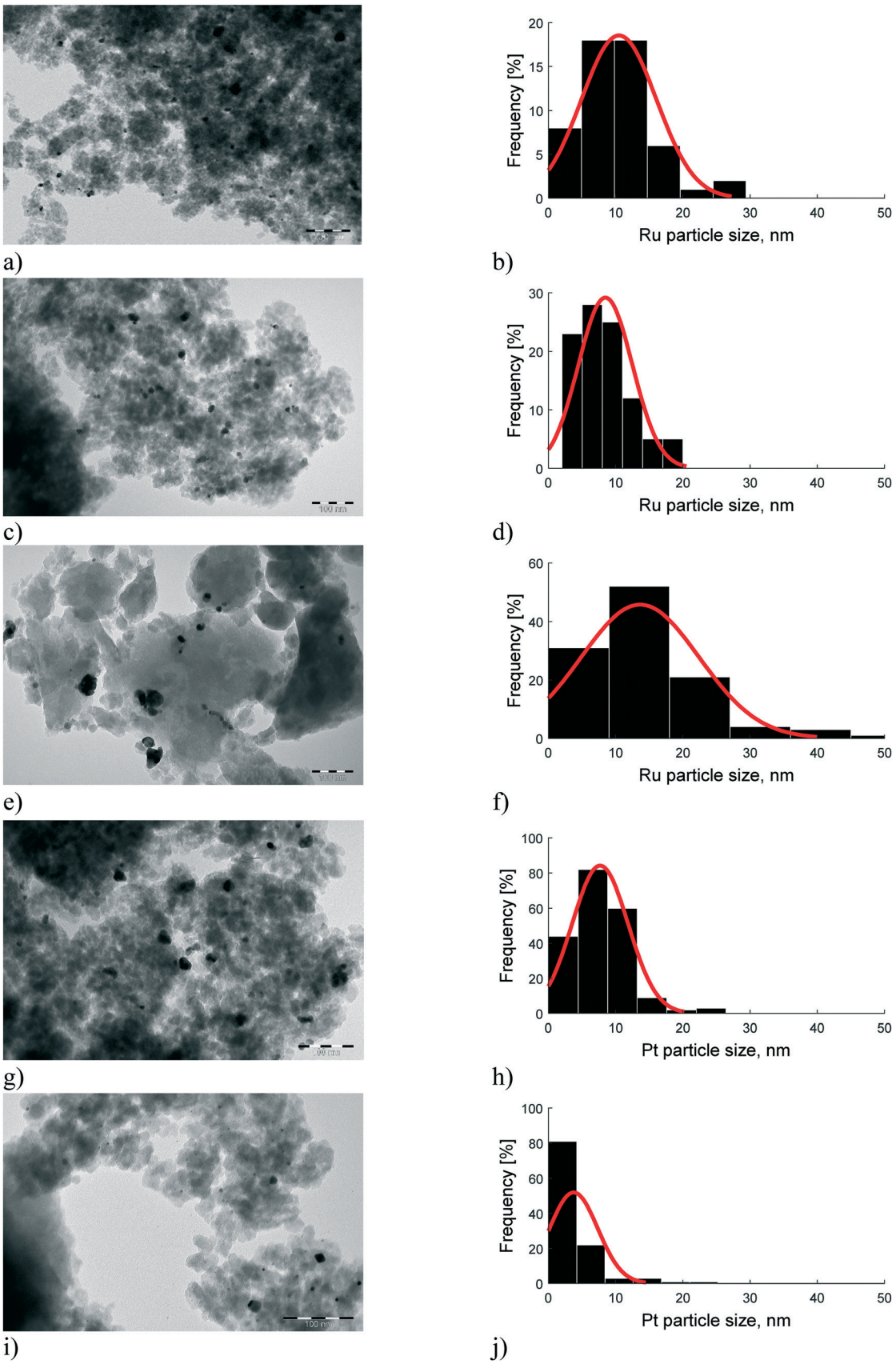

Fig. 4 TEM images and average metal particle size histograms a and b) of the fresh and c and d) spent 2 wt% [(Ru/H-beta-25) + bentonite], e and f) fresh 2 wt% Ru/H-beta-300 extrudate, g and h) the fresh and i and j) spent 2 wt% [Pt/(H-beta-25 + bentonite) *in situ*] at 35 °C under 10 bar total pressure in hydrogen.

Table 4 Average metal particle size determined from TEM images

Catalyst (extrudates)	Avg. particle size (nm)	Dispersion[a] (%)	Ref.
2.0 wt% [Ru/(H-beta-25 + bentonite)]	8	12	CW
2.0 wt% [Ru/(bentonite) + H-beta-25]	9	11	CW
2.0 wt% [Ru/(H-beta-25) + bentonite]	10 (8)	10 (12.5)	CW
2 wt% Ru/H-beta-300	12	8	CW
2.0 wt% [Pt/(H-beta-25 + bentonite) post synthesis]	7	13	8
2.0 wt% [Pt/(beta-25 + bentonite) *in situ*]	5 (2.7)	21 (37)	8 (CW)
2.0 wt% [Pt/(bentonite) + H-beta-25]	2	63	8
2.0 wt% [Pt/(H-beta-25) + bentonite]	3	29	

[a] Dispersion calculated by 100/average particle size, CW – current work, (spent catalyst).

conversion level of 80% in the batch reactor within a time interval of 13.3 min (Tables 8 and S7†).

For 2.5 wt% Pt/H-beta-25, complete conversion was achieved already at 60 min (Fig. S3c†), while 99% conversion was recorded after 150 min for 1 wt% Pt/H-beta-300 (Table S7†). On the other hand, in the trickle bed reactor, the conversion was not affected by acidity. The Ru-catalyst in the bath reactor exhibited the lowest activity giving only 80.1% after 150 min (Table S7†).

The liquid phase mass balance closure in the batch reactor varies in the range of 76.6–100% in one-pot menthol synthesis from citronellal. In the trickle bed reactor in the presence of mass transfer limitations, the GCLPA was lower than that in the batch reactor, varying in the range of 50.1–80.4% (Table 8), indicating that some heavy compounds, not visible in GC analysis, were formed.

3.4 Product distribution

Analysis of the product distribution in the trickle bed reactor especially the yields of menthols is required to understand the influence of mass transfer on selectivity. The hydrogenation *vs.* cyclization activity of the different catalysts was studied by plotting the sum of the concentrations of acyclic hydrogenation products (citronellol, nerol, geraniol, 3,7-dimethyloctanal and 3,7-dimethyloctanol, ACP) *vs.* cyclization products (pulegols and menthols, CP) in one-pot synthesis of menthol over the Pt and Ru extrudates (Fig. 7a and b). It can be seen that the highest concentrations of cyclization products were found for the 2 wt% [Pt/(H-beta-25) + bentonite] composite, which exhibits the lowest concentration of Brønsted acid sites among the three Pt-extrudates (Table 2) used in the current work. More acyclic hydrogenation products are formed over more acidic *in situ* synthesized 2 wt% [Pt/(H-beta-25 + bentonite) post synthesis] (Fig. 6a, Table 8), where Pt is located preferentially at the outer layer.[18] The lowest amount of hydrogenation products was formed with the mildly acidic synthesized 2 wt% [Pt/(H-beta-25 + bentonite) *in situ*] catalyst (Fig. 6b, Table 8). Analogous to Pt, a more prominent formation of hydrogenation products was found for more acidic 2 wt% [Ru/(H-beta-25 + bentonite), *in situ*] (Fig. 7b). There is no clear correlation for the metal dispersion in the case of Pt while for Ru extrudates the metal dispersion is the same (Table 4). Among all tested extrudates, the main products were pulegols over 2 wt% Ru/H-beta-300 (Fig. 6e) with a low amount of Brønsted acid sites and over 2 wt% [Ru/(bentonite) + H-beta-25] (Fig. 6g), which exhibits a medium amount of Brønsted acid sites, 121 μmol g_{cat}^{-1} (Table 2). These results indicate that the most important factor determining menthol production is the mild catalyst acidity in the trickle bed reactor in the presence of mass transfer limitations for the tested catalysts. Furthermore, the preparation method with

Table 5 The retention times with the molecular weights of the extracted coke from the spent catalysts 2 wt% [Ru/(H-beta-25) + bentonite] and 2 wt% [Pt/(H-beta-25 + bentonite) *in situ*] used in one-pot synthesis of menthol in a trickle bed reactor at 35 °C under 10 bar total pressure in hydrogen

2 wt% [Ru/(H-beta-25) + bentonite]			
Retention time, min	Molecular weight, g mol^{-1}	Area, %	Total area
24.18	N/A[a]	3.9	68 290
21.88	525	35.5	617 803
20.42	1050	13.6	236 361
14.96	N/A[a]	47	818 215
2 wt% [Pt/(H-beta-25 + bentonite) *in situ*]			
Retention time, min	Molecular weight, g mol^{-1}	Area, %	Total area
24.17	N/A[a]	0.1	13 318
21.85	530	3.3	799 068
14.97	N/A[a]	96.7	23 753 491

[a] The coke components eluted at 24.18 and 14.96 min in 2 wt% [(Ru/H-beta-25) + bentonite] and 24.17 and 14.97 min in 2 wt% [Pt/(H-beta-25 + bentonite) *in situ*] are very heavy molecules, N/A not available.

Table 6 CHNS results of the bifunctional platinum and ruthenium extrudates

Sample	Nitrogen (% w/w)	Carbon (% w/w)	Hydrogen (% w/w)	Sulfur (% w/w)
2.0 wt% [Ru/(H-beta-25) + bentonite]	0.03 ± 0.03	9.58 ± 0.36	1.92 ± 0.04	0.0 ± 0.0
2.0% [Pt/(H-beta-25 + bentonite) *in situ*]	0.0 ± 0.0	11.26 ± 0.48	2.12 ± 0.07	0.0 ± 0.0

the controlled metal deposition in the extrudates has a large impact on their properties and the product distribution in one-pot synthesis of menthol.

The product distribution in the batch reactor in one-pot menthol synthesis shows that the Ru-supported catalyst gave he highest yield of menthol, 72.9%, at 80% conversion (Table S7†). The lowest yield of menthol, 39.8%, was recorded for mildly acidic 1 wt% Pt/H-beta-300. In comparison, the menthol yields in the trickle bed reactor at 80% conversion were much lower than those in the batch reactor which vary in the range of 13.8–28.7%. The lowest yield of menthol, 6.6%, was obtained with the mildly acidic 2 wt% Ru/H-beta-300 which also gave the lowest conversion, 39.3%, after 90 min time-on-stream (Table 8).

To study the extent of the undesired hydrogenation reaction, the product distribution in the batch reactor was elaborated by plotting the sum of the concentrations of the undesired acyclic hydrogenation products, ACP *vs.* the sum of the concentrations of cyclization products, CP. It can be seen that nearly no acyclic hydrogenation products were formed over 2.5 wt% Ru/H-beta-300. On the other hand, 1 wt% Pt/H-beta-300 was also able to produce after prolonged times both cyclization and acyclic hydrogenation products, while over 2.5 wt% Pt/H-beta-25 the maximum amount of cyclization products was already formed during the first minute. Thereafter, more hydrogenation products were formed over this catalyst (Fig. S4†). This result indicates that the acid sites were deactivated because cyclization no longer occurs. When the current results were compared with those in ref. 4 in which the reaction was performed at 100 °C, it can be concluded that under these conditions more hydrogenation products were formed over Ru than over Pt supported H-beta zeolites. In the current case, Pt/H-beta zeolite catalysts were more active for generation of hydrogenation products in comparison to Ru/H-beta zeolites most probably due to a lower temperature at which Ru is not very active, forming acyclic hydrogenation products.

A comparison of the citronellal conversion and the menthol yield at 80% conversion as a function of acidity was made both for the trickle bed and the batch reactor (Fig. 8, Table 8, Fig. S5, Table S7†). The results clearly showed that the citronellal conversion decreased with increasing weak acid sites of extrudates in continuous operation. Higher menthol yields were obtained for the catalysts in the batch reactor under the kinetic regime. In both cases, the menthol yields slightly decreased with increasing concentration of Brønsted acid sites. The menthol yields in the current work varied in the range of 6.6* – 72.9% at 80% conversion (*at 40% conversion), which are rather low. It should, however, be kept in mind that the reaction temperature in the current case is low and in the literature a similar yield of menthols of *ca.* 70% has been reported for 1 wt% Ru/beta-25 at 100 °C under 25 bar hydrogen.[4] Meanwhile higher values exceeding 90% were obtained over 2 wt% Pt/H-beta in 1,4-dioxane as a solvent at 80 °C under 20 bar hydrogen.[5] Higher values of menthol yields (85–96%) were published in the literature[8,14] for Ru- and Pt-catalysts in a batch reactor under higher temperature (60–80 °C) and higher pressure (20 bar) conditions.

Elucidation of stereoselectivity to menthol at 80% conversion for both for the trickle bed and batch reactors showed that in the former case it varied between 66.8 and 72.9% (Table 8) and 70.2–71.3% in the batch reactor (Table S7†). Slightly lower stereoselectivity was observed for Ru-beta-bentonite extrudates compared to Pt-beta-bentonite (Table 8). The stereoselectivity to menthols at 80 °C under 20 bar hydrogen was 76.3% over 2 wt% Pt/H-beta in dioxane as a solvent after 12 h at conversion higher than 99%.[5] For the Ru/H-beta-300 catalyst without a binder, the stereoselectivity to menthol was higher in the batch reactor (83.1%) in comparison with the results obtained over extrudates in the trickle bed reactor (74.9%) at 40% conversion. It can be concluded that a similar stereoselectivity to menthol was obtained under the kinetic regime in the batch reactor and in the trickle bed reactor under mass transport limitations at higher conversion. One of the explanations is that the cyclization diastereoselectivity is determined by thermodynamics.[6,19,25]

When comparing the stereoselectivity to menthol reported in the literature[4] over Ru/H-beta-35, 75% stereoselectivity to menthol at nearly full conversion was obtained after 180 min.[4] It should be pointed out that the results are not directly comparable, because in the literature[4] the reaction was performed at 100 °C under 25 bar using a citronellal to

Table 7 Crushing strength of extrudates in vertical and horizontal positions

Extrudates	Vertical MPa	Horizontal MPa	Ref.
Ru/(H-beta-25 + bentonite)	4.14 ± 0.24	1.00 ± 0.20	CW
Ru/(bentonite) + H-beta-25	3.96 ± 0.14	0.86 ± 0.10	
Ru/(H-beta-25) + bentonite	3.15 ± 0.12	1.20 ± 0.33	
Ru/H-beta-300			
Pt/(H-beta-25 + bentonite) post synthesis	4.77 ± 0.16	1.24 ± 0.19	8
Pt/(H-beta-25 + bentonite) *in situ*	4.45 ± 0.21	0.77 ± 0.25	
Pt/(bentonite) + H-beta-25	3.64 ± 0.21	0.76 ± 0.08	
Pt/(H-beta-25) + bentonite	3.24 ± 0.21	0.68 ± 0.14	

MTL – metal: Pt or Ru, CW – current work.

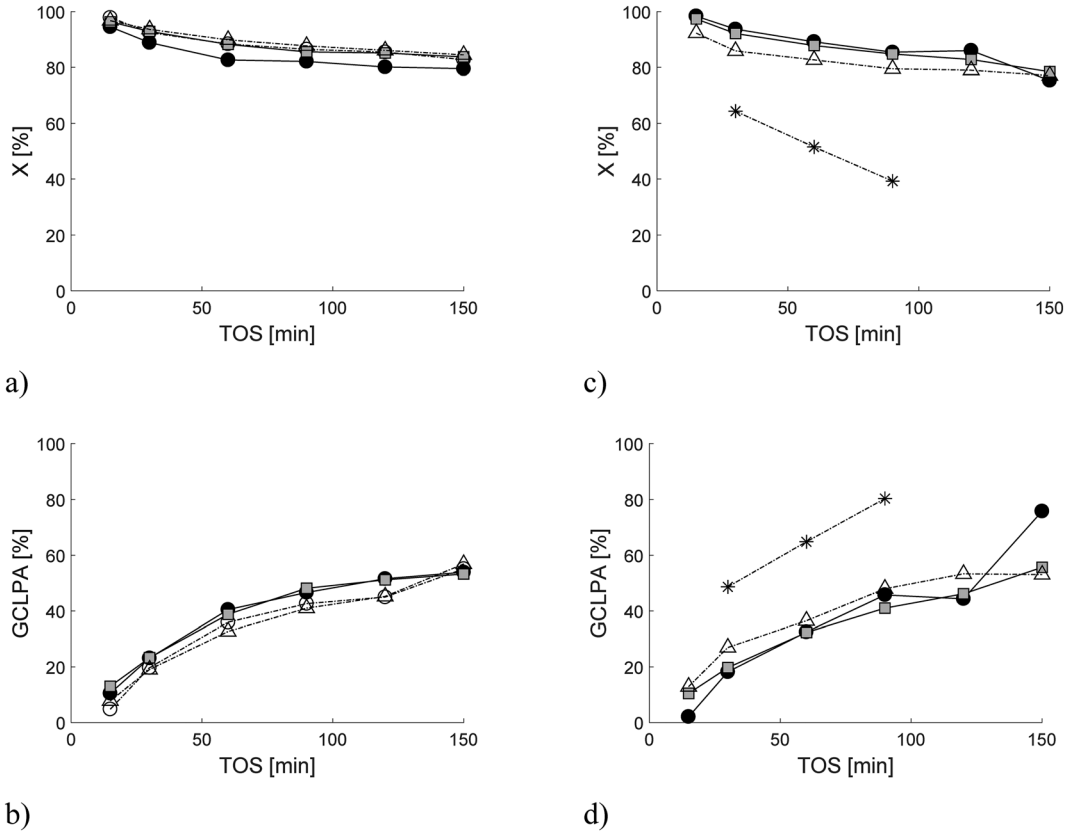

Fig. 5 For Pt extrudates: a) conversion and b) liquid phase mass balance for (○) 2 wt% [Pt/(H-beta-25 + bentonite) post synthesis], (●) 2 wt% [Pt/(H-beta-25 + bentonite) *in situ*], (■) 2 wt% [Pt/(bentonite) + H-beta-25], and (△) 2 wt% [Pt/(H-beta-25) + bentonite]. For Ru extrudates: c) conversion and d) liquid phase mass balance for (*) 2 wt% Ru/H-beta-300, (●) 2 wt% [Ru/(H-beta-25 + bentonite) *in situ*], (■) 2 wt% [Ru/(bentonite) + H-beta-25], and (△) 2 wt% [Ru/(H-beta-25) + bentonite].

catalyst mass ratio of 9 : 1, whereas in the current case the reaction was performed at 10 bar total pressure in a H_2 atmosphere and 35 °C with a citronellal to catalyst mass ratio of 1.2 : 1. In the current work using 2.5 wt% Ru/H-beta-300 with

Table 8 Results from one pot synthesis of menthol from citronellal in a continuous reactor at 35 °C under 10 bar total pressure in H_2. Conversion of citronellal (*X*) and liquid phase mass balance (GCLPA) are given at 150 min time-on-stream. Yields (*Y*) of different products, stereoselectivity (SS) and reaction rate (*r*) are given at 80% conversion. Conditions: the amount of catalyst 1 g, the initial citronellal concentration 0.086 M

Catalyst (extrudates)	X %	GCLPA	Y_{Ps}	Y_{MEs}	Y_{ACS}	Y_{DM}	Y_{CS}/Y_{ACS} —	SS_{IP} %	SS_{ME}	r mol s^{-1} g	η —	TOF s^{-1}	PCU %
2 wt% [Pt/(H-beta-25 + bentonite) post]	82.8	50.1	0	14.4	18.2	2.2	0.6	0.0	71.3	5.63×10^{-7}	0.13	0.053[a]	46.3[a]
2 wt% [Pt/(H-beta-25 + bentonite) *in situ*]	79.6	52.9	0.2	18.2	10.8	0.3	1.7	0.0	70.6	5.20×10^{-7}	0.12	0.022	18.8
2 wt% [Pt/(bentonite) + H-beta-25]	83.8	51.9	0.4	23.1	16.8	0.2	0.9	0.0	72.9	6.23×10^{-7}	0.14	0.011	9.2
2 wt% [Pt/(H-beta-25) + bentonite]	84.5	51.6	0.8	28.7	16.2	2.4	1.8	0.0	71.6	6.44×10^{-7}	0.14	0.013	11.2
2 wt% [Ru/(H-beta-25 + bentonite) *in situ*]	75.4	67.6	14.9	17.2	0.7	1.4	48.7	61.9	67.8	8.83×10^{-7}	—	0.031	—
2 wt% [Ru/(bentonite) + H-beta-25]	78.5	54.3	17.2	12.5	0.2	0.0	120.0	62.4	68.5	9.03×10^{-7}	—	0.030	—
2 wt% [Ru/(H-beta-25) + bentonite]	77.1	51.9	11.2	13.8	0.2	0.3	109.9	60.8	66.8	6.47×10^{-7}	—	0.019	—
2 wt% Ru/H-beta-300	39.3[b]	80.4[b]	12.8[c]	6.6[c]	0.3[c]	0.0[c]	69.8[c]	65.2[c]	74.9[c]	2.71×10^{-7}[c]	0.06[c]	0.016[c]	3.7[c]

[a] Based on recalculated Pt concentration in the entire extrudate body. [b] 90 min TOS. [c] At 39.3% conversion. Ps – pulegols = isopulegol (IP) + neoisopulegol (NIP) + isoisopulegol (IIP) + neoisoisopulegol (NIIP), MEs – menthols: menthol (ME) + neomenthol (NME), CS – cyclic products: pulegols + menthols, ACS – acyclic monomeric products: citronellol (CLOL) + 3,7-dimethyloctanal (DMA) + 3,7-dimethyloctanol (DMO) + nerol (NRL) + geraniol (GRN), DM – dimeric ethers, SS_{IP} – stereoselectivity of isopulegol = IP/$\sum$Ps, SS_{ME} – stereoselectivity of menthol = ME/$\sum$MEs, η – effectiveness factor: for 2 wt% Pt extrudates, it was calculated as a ratio of the reaction rate of extrudates at 80% conversion and the reaction rate of the 2.5 wt% Pt/H-beta-25 powder catalyst at 80% conversion (Table S7); for 2 wt% Ru/H-beta-300 extrudates, it was calculated as a ratio of the reaction rate of extrudates at 39.3% conversion and the reaction rate of the 2.5 wt% Ru/H-beta-300 powder catalyst at 40% conversion (Table S7), TOF – turnover frequency, PCU – percentage of catalyst utilisation: for 2 wt% Pt extrudates, it was calculated as a ratio of TOF of extrudates in the trickle-bed reactor and TOF of the 2.5 wt% Pt/H-beta-25 powder catalyst in the batch reactor at 80% conversion (Table S7); for 2 wt% Ru/H-beta-300 extrudates, it was calculated as a ratio of TOF of extrudates in the trickle-bed reactor and TOF of the 2.5 wt% Ru/H-beta-300 powder catalyst in the batch reactor at 40% conversion (Table S7).

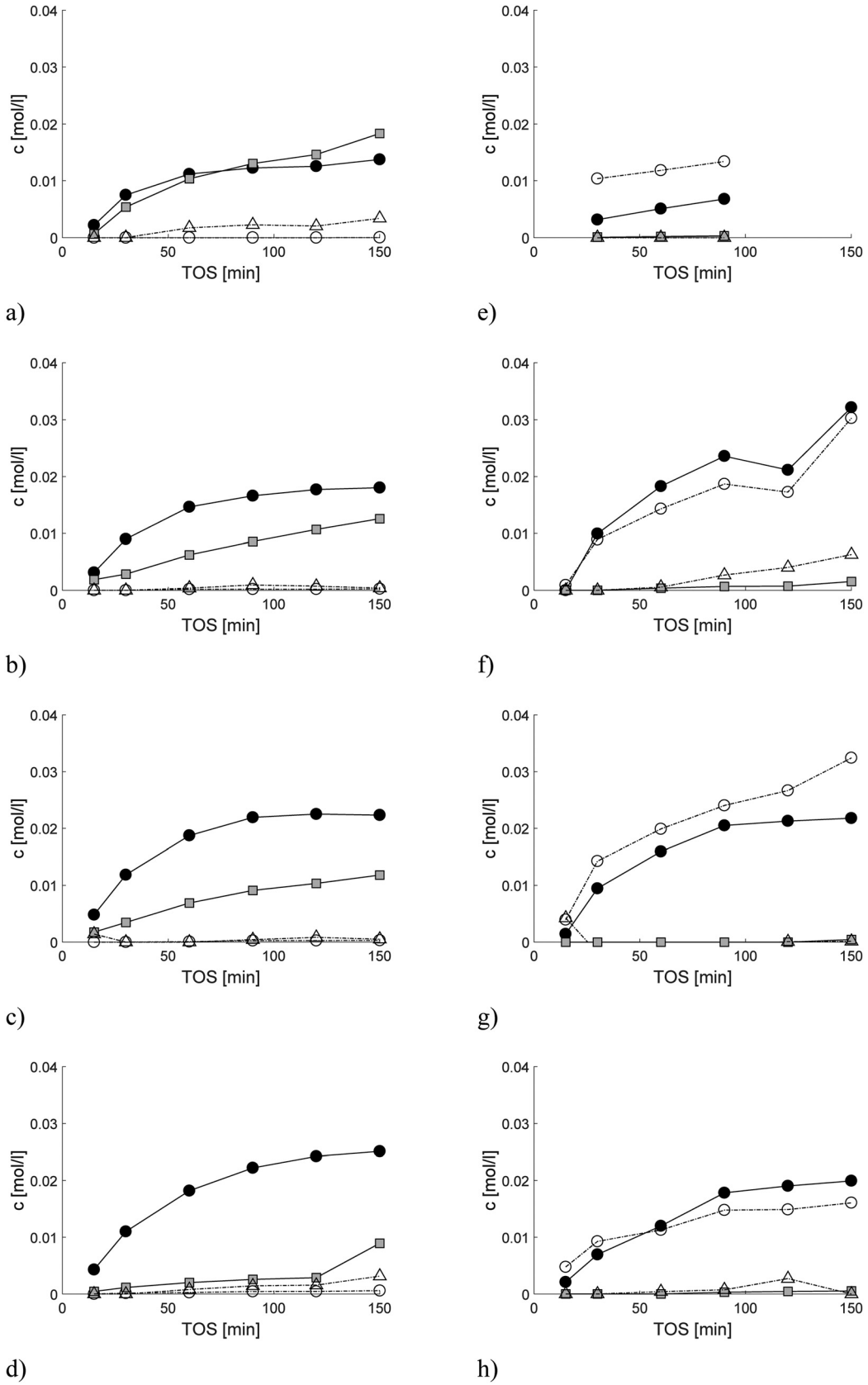

Fig. 6 Concentration of products in continuous one-pot synthesis of menthol over extrudates: a) 2 wt% [Pt/(H-beta-25 + bentonite) post synthesis], b) 2 wt% [Pt/(H-beta-25 + bentonite) *in situ*], c) 2 wt% [Pt/(bentonite) + H-beta-25], d) 2 wt% [Pt/(H-beta-25) + bentonite], e) 2 wt% Ru/H-beta-300, f) 2 wt% [Ru/(H-beta-25 + bentonite) *in situ*], g) 2 wt% [Ru/(bentonite) + H-beta-25], and h) 2 wt% [Ru/(H-beta-25) + bentonite]. Notation: (○) pulegols, (●) menthols, (■) acyclic monomeric hydrogenation products and (△) dimeric ethers.

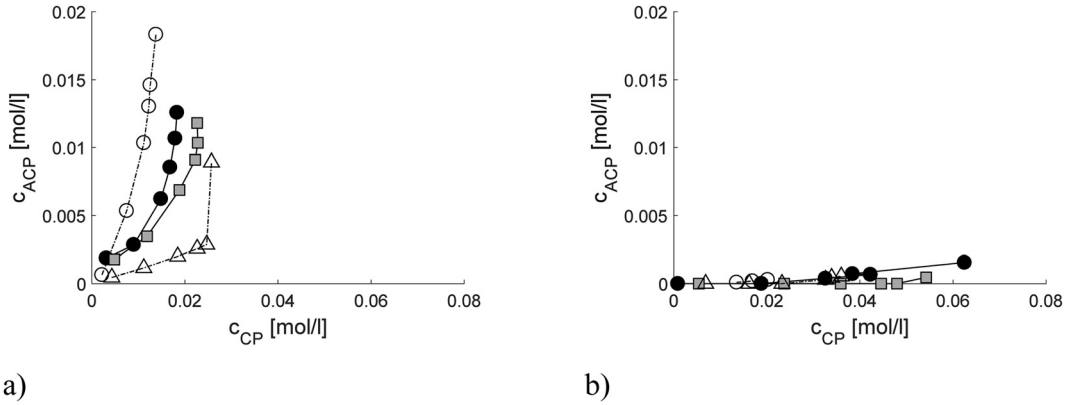

Fig. 7 Concentration of acyclic monomeric hydrogenation products (ACP) *vs.* cyclic products (CP) in continuous one-pot synthesis of menthol over extrudates: a) (○) 2 wt% [Pt/(H-beta-25 + bentonite) post synthesis], (●) 2 wt% [Pt/(H-beta-25 + bentonite) *in situ*], (■) 2 wt% [Pt/(bentonite) + H-beta-25], and (△) 2 wt% [Pt/(H-beta-25) + bentonite]; b) (○) 2 wt% Ru/H-beta-300, (●) 2 wt% [Ru/(H-beta-25 + bentonite) *in situ*], (■) 2 wt% [Ru/(bentonite) + H-beta-25], and (△) 2 wt% [Ru/(H-beta-25) + bentonite].

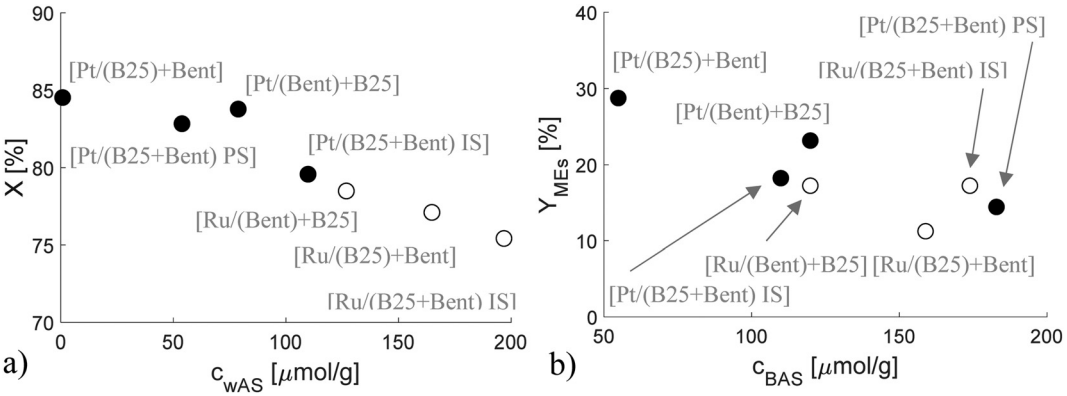

Fig. 8 a) Conversion of citronellal as a function of weak acid sites of different extrudates, b) the yield of menthols at 80% conversion as a function of Brønsted acid sites of different extrudates. Notation: B25 – H-beta-25, Bent – bentonite, IS – *in situ*, PS – post synthesis.

a rather large size of Ru particles (17 nm) 80% conversion was obtained with 71.3% stereoselectivity to menthol after 150 min. When comparing the current results with those in the literature,[4] the effect of metal particle size on stereoselectivity cannot be elucidated. Higher values of stereoselectivity to the desired (−)-menthol (80–85%) were observed over Cu/SiO_2, Pd–$H_3PW_{12}O_{40}/SiO_2$ and a MOF catalyst containing coordinatively unsaturated Cr^{3+} sites and palladium nanoparticles at 50–90 °C, 8–50 bar after 2–18 h in a batch reactor.

3.5 Regeneration and reuse of Ru/H-beta-300 in the trickle bed reactor

A regeneration test of 2 wt% Ru/H-beta-300 extrudates was performed in the trickle bed reactor (Fig. 9). The results showed that both the conversion and the liquid phase mass balance were very similar in the second experiment, prior to which, the reactor was flushed with cyclohexane for 30 min. This is a promising result clearly showing the reusability of Ru based extrudates. Further studies should be made with a longer time-on-stream in order to demonstrate the long-term stability of the catalyst, especially with Pt catalysts, which exhibited better stability than mildly acidic 2 wt% Ru/H-beta-300 extrudates (Fig. 6 and 9).

4 Conclusions

One-pot menthol synthesis was investigated in a trickle bed reactor with Ru/H-beta-300 extrudates without a binder and Pt- and Ru-extrudates prepared from 70 wt% H-beta-25 zeolite and 30 wt% bentonite with controlled deposition of the metal either on the zeolite or the binder. The catalyst characterization results revealed that the method of the extrudate synthesis has a major impact especially on the acidity, metal dispersion and distribution of the metal in the extrudates. The catalyst, prepared by loading Pt on H-beta-bentonite extrudates, exhibited an egg-shell structure and the highest Brønsted acidity among Pt extrudates. The highest Brønsted acidity was found in extrudates prepared from the Ru/H-beta-25-bentonite composite, which was then extruded, and the lowest one was observed for extrudates prepared from Pt/H-beta-25 mixed with bentonite and then extruded.

In one-pot synthesis of menthol from citronellal in the trickle bed reactor, conversions of citronellal were nearly the

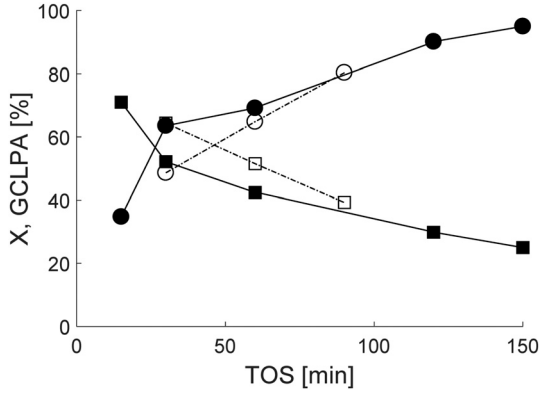

Fig. 9 Conversion, X (■) and liquid phase mass balance, GCLPA (●) in one-pot synthesis of menthol starting from citronellal at 35 °C under 10 bar total pressure in H_2 over 2 wt% Ru/H-beta-300 extrudates. Symbols: fresh catalyst (open symbol), reused catalyst (closed symbol).

same for Pt extrudates, being independent from the catalyst acidity or the metal particle size. The same is valid for Ru extrudates, except for the very mildly acidic Ru/beta-300 extrudate without a binder, which gave much lower conversion. Pt extrudates showed better stability with time on stream in comparison to Ru extrudates. Oligomer formation occurred during menthol synthesis despite a low reaction temperature, 35 °C, resulting in incomplete liquid phase mass balance closure.

Deactivated ruthenium catalysts could be, however, regenerated by washing the catalyst with cyclohexane as illustrated for Ru/H-beta-300 extrudates.

The highest menthol yield was obtained with the mildly acidic catalysts for Pt and Ru extrudates in the trickle bed reactor with a significant influence of mass transfer and an analogous trend was observed in the kinetic experiments performed in a batch reactor. Hydrogenation was more prominent for Pt than for Ru catalysts, most probably due to their high hydrogenation ability already at 35 °C. Stereoselectivity to menthols, defined as menthol/(neomenthol + menthol) × 100, varied in the trickle bed reactor in the range of 67 to 73%, while in the batch reactor for Ru- and Pt-catalysts it was in the range of 70–71% independent of support acidity.

The best catalyst in the form of extrudates giving the highest menthol yield and a low amount of acyclic hydrogenation products was Ru-beta-bentonite where Ru was located randomly in the mixture of 70% H-beta-25 and 30% bentonite binder.

Conflicts of interest

There are no conflicts of interest to declare.

Acknowledgements

The authors are grateful to the Academy of Finland for funding through the project: Synthesis of spatially controlled catalysts with superior performance.

References

1 G. P. P. Kamatou, I. Vermaak, A. M. Viljoen and B. M. Lawrence, *Phytochemistry*, 2013, **96**, 15–25.
2 B. M. Lawrence, *Mint: The Genus Mentha*, CRC Press, Boca Raton, 2006.
3 C. B. Cortes, V. T. Galvan, S. S. Pedro and T. V. Garcia, *Catal. Today*, 2011, **172**, 21–26.
4 J. Plösser, M. Lucas and P. Claus, *J. Catal.*, 2014, **320**, 189–197.
5 P. Mertens, F. Verpoort, A. N. Parvulescu and D. de Vos, *J. Catal.*, 2006, **243**, 7–13.
6 P. Mäki-Arvela, N. Kumar, V. Nieminen, R. Sjöholm, T. Salmi and D. Yu. Murzin, *J. Catal.*, 2004, **225**, 155–169.
7 J. Plößer, M. Lucas, J. Wärnå, T. Salmi, D. Yu. Murzin and P. Claus, *Org. Process Res. Dev.*, 2016, **20**, 1647–1653.
8 J. ten Dam, A. Ramanathan, K. Djanashvili, F. Kapteijn and U. Hanefeld, *RSC Adv.*, 2017, **7**, 12041–12053.
9 F. G. Cirujano, F. Xamena and A. Corma, *Dalton Trans.*, 2012, **41**, 4249–4254.
10 F. Neatu, S. Coman, V. I. Parvulescu, G. Poncelet, D. De Vos and P. Jacobs, *Top. Catal.*, 2009, **52**, 1292–1300.
11 I. B. Adilina, Tasfir, J. A. Laksmono and E. Agustia, *Jurnal Teknologi Industri Pertanian*, 2007, **17**, 69–73.
12 A. Corma and M. Renz, *Chem. Commun.*, 2004, 550–551.
13 L. Alaerts, E. Seguin, H. Poelman, F. Thibault-Starzyk, P. A. Jacobs and D. E. De Vos, *Chem. – Eur. J.*, 2006, **12**, 7353–7363.
14 C. Milone, C. Gangemi, G. Neri, A. Pistone and S. Galvagno, *Appl. Catal., A*, 2000, **199**, 239–244.
15 K. A. D. Rocha, P. A. Robles-Dutenhefner, E. M. B. Sousa, E. F. Kozhevnikova, I. V. Kozhevnikov and E. V. Gusevskaya, *Appl. Catal., A*, 2007, **317**, 171–174.
16 Y. T. Nie, W. Niah, S. Jaenicke and G. K. Chuah, *J. Catal.*, 2007, **248**, 1–10.
17 N. Ravasio, N. Poli, R. Psaro, M. Saba and F. Zaccheria, *Top. Catal.*, 2000, **13**, 195–199.
18 Z. Vajglová, N. Kumar, M. Peurla, L. Hupa, K. Semikin, D. A. Sladkovskiy and D. Y. Murzin, *Ind. Eng. Chem. Res.*, 2019, **58**, 10.
19 Z. Vajglová, N. Kumar, P. Mäki-Arvela, K. Eränen, M. Peurla, L. Hupa, M. Nurmi, M. Toivakka and D. Y. Murzin, *Ind. Eng. Chem. Res.*, 2019, **58**, 18084–18096.
20 Z. Vajglová, N. Kumar, P. Mäki-Arvela, K. Eränen, M. Peurla, L. Hupa and D. Y. Murzin, *Org. Process Res. Dev.*, 2019, DOI: 10.1021/acs.oprd.9b00346, in print.
21 D. Y. Murzin, *Engineering Catalysis*, Walter de Gruyter, Gottingen, 2013.
22 C. A. Emeis, *J. Catal.*, 1993, **141**, 347–354.
23 H. A. Abdullah, A. Hauser, F. A. Ali and A. Al-Adwani, *Energy Fuels*, 2006, **20**, 320–323.
24 Z. Vajglová, N. Kumar, M. Peurla, J. Peltonen, I. Heinmaa and D. Y. Murzin, *Catal. Sci. Technol.*, 2018, **8**, 6150–6162.
25 N. Ravasio, M. Antenori, F. Babudri and M. Gargano, *Stud. Surf. Sci. Catal.*, 1997, **108**, 625–632.